COMMUNICATIONS
FROM THE
UNIVERSITY OF LONDON
OBSERVATORY
No. 56

MEASUREMENT OF TRANSITION PROBABILITIES IN THE Cl I, II AND C I SPECTRA

by

E. W. FOSTER

Reprinted from

PROCEEDINGS OF THE PHYSICAL SOCIETY

Vol. 80, pp. 882–893, 1962

PROC. PHYS. SOC., 1962, VOL. 80

Measurement of Transition Probabilities in the Cl I, II and C I Spectra

By E. W. FOSTER

University of London Observatory, Mill Hill Park, N.W.7.†

MS. received 29th May 1962

Abstract. Using a vortex-stabilized arc in chloroform, transition probabilities have been obtained for all classified Cl I lines from 3900–5200 Å and for the strongest Cl II lines in this region. New C I measurements are reported in satisfactory agreement with means from previous works. A strong continuum associated with the chloroform plasma is attributed mainly to the Cl I recombination spectrum in the 3900–5200 Å region. Transition probabilities for Cl lines average 23% above those of Hey.

§ 1. INTRODUCTION

TRANSITION probabilities have been measured in Cl I and II by Hey (1959) and in C I by Maecker (1953), Richter (1958) and Foster (1962, to be referred to as I).

The primary objective of this work was the further determination of chlorine transition probabilities previously measured only for three lines of Cl I and one of Cl II. Experimentally, chlorine is of interest because of the number of stable volatile metallic and other chlorides.

Basic types of light source suitable for this project were the liquid vortex and solid wall stabilized arcs (Maecker 1951, 1956); considerations, governing our choice of the first mentioned, follow.

The liquid vortex arc produces more gas turbulence than the wall-stabilized type. Both types possess a large radial temperature gradient which may cause thermal diffusion and other undesirable plasma component separation effects. These are at least reduced, if not eliminated under our conditions, by the greater mixing of gas with the liquid vortex arc. Against this advantage is set the disadvantage of greater wobble of the arc column than obtains with wall stabilization. However, if the wobble is small it can be tolerated and some correction can be applied for the resulting defect in the axial emission relative to that from a steady plasma column (I). But with the possibility remaining of residual wobble and/or plasma separation errors, pure chloroform was chosen as the vortex fluid for this work. This enabled the C I spectrum to be excited under good conditions simultaneously with those of Cl I, II and H. C I transition probabilities were derived independently and compared with existing data; agreement guards empirically against serious error in the chlorine measurements.

For the very steady wall-stabilized arcs attempts have recently been made to calculate certain separation effects (Frie and Maecker 1961). Notwithstanding excellent progress Richter (1961) maintains that it is not usually possible to make the correction very accurately.

† Experimental work done at Imperial College in 1959.

§ 2. EXPERIMENTAL

2.1. *Light Sources, Optics, Spectrograph*

Details of the arc chamber used have been given in I. The arc, operated at 52–69 amp d.c. was viewed end-on as before. Phosgene and other heavy noxious vapours were produced from the chloroform and partially removed by a fume extractor but an old Service respirator gave full protection.

The Euler (1953a, b) carbon arc with a 5 mm Ringsdorff Spektral II anode was the photometric standard.

The spectrograph and optics of Foster (1958) were used. The spectrograph is a photoelectric recording machine for absolute intensity measurement. It is normally used at a resolving power of about 3000 which produces a useful instrumental broadening unless close lines have to be resolved.

2.2. *The Recordings and their Measurement*

Chloroform and adjacent comparison spectra were recorded on 6 feet of Ilford 5G91 70 mm film from 3850–6600 Å with a dispersion varying from 1·92–1·89 Å mm^{-1}. The scanning rate was about 186 Å sec^{-1} so that a recording required 15 sec. The total running time for the chloroform arc was 45 sec per recording; 30 sec were required for checking operating conditions and for the attainment of steady conditions in the light path through the electrodes.

Measurement has been facilitated and accuracy improved firstly by making indirect instead of direct measurements from the film, which is now projected on to graph paper using a distortion-free photographic enlarger. The spectrum, now magnified to 2 mm $Å^{-1}$, is traced out. Secondly, a machine is used to rectify sections (strong line peaks) recorded at reduced sensitivity; this is a specially constructed pantograph which moves over the spectrum trace on rails parallel to the wavelength axis, the pantograph action occurring perpendicularly.

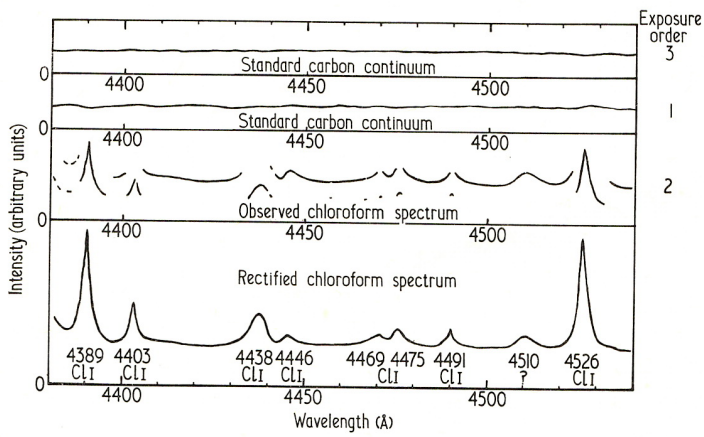

Figure 1. Typical example of recorded and rectified spectrum.

Original and rectified traces of parts of the chloroform spectrum are shown in figure 1. Corrections, arising especially because of the optics geometry needed to observe a long thin plasma filament end-on, must be applied to the simple $CHCl_3/C$ deflection ratio to render the chloroform intensities absolute. The resultant correction

factor F_λ for this set-up was derived in I for arcs in steam, etc. and is similar here apart from effects resulting from the radial intensity distribution having about twice the breadth measured for steam. Here $1{\cdot}06 \leqslant F_\lambda \leqslant 1{\cdot}09$ compared with $1{\cdot}17 \leqslant F \leqslant 1{\cdot}25$ formerly. Possibly excepting H_α, which was not used, all lines were optically thin.

2.3. *Treatment of Unresolved Lines and Weak Lines*

The low resolving power (§ 2.1) rendered the occurrence of several unresolved blends inevitable. In these, as in other cases, only the total absolute intensity was measured (by planimeter).

To assign intensities for such Cl I blends, Kiess's (1933) visual scale intensities were used. Figure 2 shows Kiess's data plotted against our photoelectric absolute intensities. The precision of Kiess's scale becomes evident from the log plot.

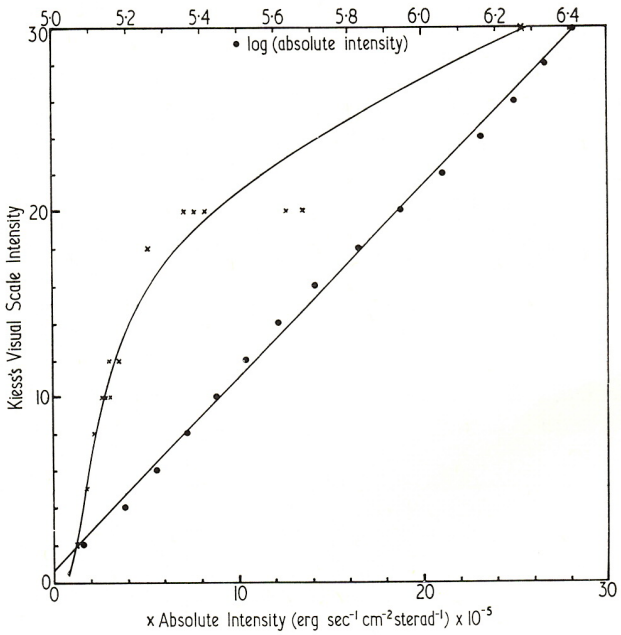

Figure 2. Kiess's (1933) visual scale intensities on an absolute scale. The absolute intensities refer to an 18·5 mm plasma column measured end-on.

By this combination of high resolution relative photographic and low resolution absolute photoelectric measurements, absolute intensities were assigned with fair certainty to most blend components. Figure 2 also makes possible the assignment of absolute intensities to weak lines observed photographically by Kiess but undetected or too weak to measure here.

This procedure would hardly be possible but for the circumstance that the upper states of nearly all the Cl I lines observed have about the same excitation potential, so that any difference between the 'temperature' of Kiess's source and ours should not produce much error. The Kiess excitation mechanism no doubt differed from ours but figure 2 does not give much indication of non-thermal behaviour.

§ 3. REDUCTIONS

Thermal equilibrium and thorough mixing of the chloroform dissociation products is assumed. Equations similar to (1)–(5) of I can then be written down to describe the particle equilibrium at temperature T and pressure P (atmospheric) for a plasma of chemical composition $CHCl_3$ at room temperature.

From these equations we can derive the eliminant

$$\{bd'-c(c'-c)\}\{(c'-c)-b(b'-b)\} = \{c(b'-b)-d'\}^2 \tag{1}$$

to determine the neutral hydrogen atom density $n_N{}^H$. This is equation (7) of I but the symbols now take the meanings

$$\left.\begin{aligned} b &= 5n_N{}^H - N & b' &= S^C + 2S^{Cl} \\ c &= 5S^H n_N{}^H & c' &= 2S^{Cl}S^C - NS^{Cl} + n_N{}^H(2S^{Cl} - S^C - S^H) \\ & & d' &= n_N{}^H(S^H S^{Cl} + S^C S^{Cl} - 2S^H S^C) - NS^{Cl}S^C \end{aligned}\right\} \tag{2}$$

with $N = P/kT$ and S^H, S^C, S^{Cl} the Saha functions $S(T)$ for neutral hydrogen, carbon and chlorine at temperature T where

$$S(T) = \frac{(2\pi mkT)^{3/2}}{h^3}\frac{2Z_i}{Z_N}\exp\left[\frac{-E-\Delta E}{kT}\right] \tag{3}$$

Z is the partition function of the neutral atom (N) or ion (i), E the ionization energy of neutral atom,

$$\Delta E = 7 \times 8068 \times 10^{-7}\sqrt[3]{n_e}hc \text{ erg}, \tag{4}$$

and n_e is the electron density.

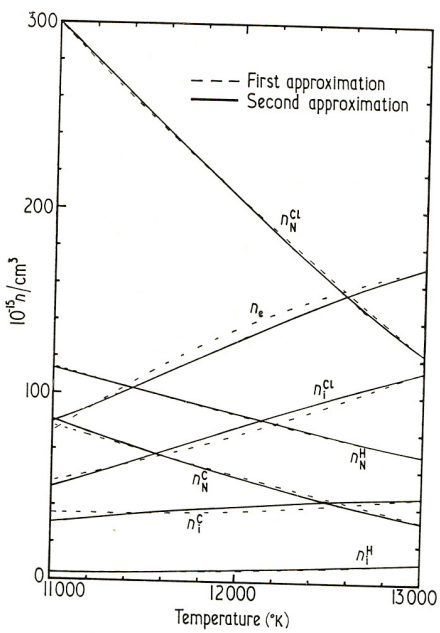

Figure 3. Particle density as a function of temperature in chloroform plasma.

A 40% underestimated n_e for Unsöld's (1948) correction ΔE enabled a proper solution of equation (1) for $n_N{}^H$ to be found numerically. The other particle densities including n_e were then readily obtained to a first approximation. This n_e was then put into the Saha functions in equations (2) and an iteration performed on the solution of equation (1). Results are shown in figure 3.

We shall not repeat details of the derivation of the transition probabilities $A_n{}^m$, beyond saying that H_β and H_γ absolute intensities determined the gas temperature, which could be read off from the computed curve shown in figure 4 (cf. I, figure 6). Transition probabilities of C I and Cl I and II lines were obtained from computed curves of the functions $\int I(\bar{\nu})d\bar{\nu}/n^P A_n{}^m$ against T, figures 5, 6, and 7, and a knowledge of T and the absolute intensities.

§ 4. RESULTS

Transition probabilities $A_n{}^m$ (m refers to the upper and n to the lower state) and gf-values tabulated below are mostly means from independent reductions of seven chloroform arc recordings with gas temperatures in the range 11 177–11 617 °K. The expression $|gf|$ is symmetrical in the upper and lower states. Thus, if f_{abs} and f_{em} are respectively the absorption and emission oscillator strengths for the transition in question and g refers to the statistical weight of the state, we have $-g_m f_{em} = g_n f_{abs} = |gf|$.

The continuum intensity is derived from the same recordings grouped now into two sets, for each of which an average temperature is extracted.

Chloroform continuum

The thick lines in figure 8 show the end-on continuous emission. The standard carbon emission has been added for comparison (see below for computed continua).

Table 1

Comparison of C I Transition Probability Measurements and Recommended Mean Values. The gf-values.

(1)	(2)	(3)	(4)	(5)	(6)	(7)	(8)
5380·242	7·1	12·5	12·0 ±9%	11·5 ±6%	10·5	10·8	14·1
5052·122	8·6	13·0	16·1 ±8%	12·7 ±4%	12·6	12·6	24·1
5040	1·5	3·0	2·09 ±7%	1·34 ±13%	2·2	2·0	11·4
4932·00	15	35·0	46·3 ±5%	34·0 ±6%	32	33	12·1
4826·73	—	—	—	3·4 ±12%	—	—	—
4770	5·2	12·0	12·6 ±8%	9·5 ±2%	9·9	9·8	30·1
4371·33	—	—	—	4 Bl	—	—	—
4268·99	—	—	—	2·3 ±8%	—	—	—

(1) Wavelength (Å); (2)–(7) $A_n{}^m \times 10^{-5}$ ($A_n{}^m$ in sec^{-1}); (2) Maecker 1953; (3) Richter 1958; (4) Foster 1962; (5) this work; (6) previously recommended mean values (I); (7) new recommended means from all data; (8) $|gf| \times 10^3$, new recommended means from all data. Tolerances are probable errors from scatter. Bl, extracted from blend with Cl I λλ 4371·55 and 4369·52 after our absolute equivalent of Kiess's intensity (figure 2) had been subtracted from our absolute intensity for the blend; see note 13, table 2. λλ 5040 and 4770 data refer to complete multiplets (I). For details of transitions see Moore 1945.

Table 2

Cl I Transition Probabilities A_n^m and *gf*-values (A_n^m in sec^{-1})

λ (Å)	Intensity K	Transition (Kiess 1933) n	m	$10^{-5}A_n^m$	$10^3\|gf\|$	Notes (1)
5140·35	(5)	$4s\ ^2P_{1/2}$	$4p'\ ^2P_{3/2}^0$	2·46	3·90	K; n
5099·80	(8)	$4s\ ^2P_{1/2}$	$4p'\ ^2P_{1/2}^0$	8·46	6·60	K: (2)
4976·62	(10)	$4s\ ^2P_{3/2}$	$4p'\ ^2P_{3/2}^0$	4·03 ±8%	5·98	
4852·70	(8)	$4s\ ^2P_{3/2}$	$5p\ ^4D_{5/2}^0$	2·17	4·60	K: n.o. (3)
4818·64	(2)	$4s\ ^2P_{1/2}$	$5p\ ^4S_{3/2}^0$	1·86	2·60	K: 29·4% (4)
4818·42	(3)	$4s\ ^2P_{3/2}$	$5p\ ^4P_{1/2}^0$	3·94	2·75	K: 33·8% (4)
4796·76	(2)	$4s\ ^2P_{1/2}$	$5p\ ^2D_{3/2}^0$	1·93	2·67	K: 20·7% (5)
4740·71	(10)	$4s\ ^2P_{3/2}$	$5p\ ^4D_{3/2}^0$	4·53 ±7%	6·11	
4721·24	(8)	$4s\ ^2P_{3/2}$	$5p\ ^2D_{5/2}^0$	2·23 ±7%	4·48	
4691·53	(12)	$4s\ ^2P_{3/2}$	$5p\ ^4D_{1/2}^0$	10·80 ±7%	7·14	
4677·76	(7)	$4s\ ^2P_{3/2}$	$5p\ ^2S_{1/2}^0$	5·20 ±18%	3·42	B
4674·40	(2)	$4s\ ^2P_{3/2}$	$5p\ ^4S_{3/2}^0$	1·81	2·37	K: n
4661·22	(18)	$4s\ ^2P_{1/2}$	$5p\ ^2P_{3/2}^0$	8·46 ±5%	11·0	
4654·05	(10)	$4s\ ^2P_{3/2}$	$5p\ ^2D_{3/2}^0$	4·67 ±9%	6·08	
4623·96	(10)	$4s\ ^2P_{1/2}$	$4p'\ ^2D_{3/2}^0$	4·38 ±7%	5·62	
4601·00	(20)	$4s\ ^2P_{1/2}$	$5p\ ^2P_{1/2}^0$	42·1 ±3%	26·7	H
4580·47	(3)	$4s\ ^4P_{3/2}$	$4p'\ ^2P_{3/2}^0$	1·75	2·20	K: n
4578·17	(4)	$4s\ ^4P_{1/2}$	$5p\ ^4P_{3/2}^0$	1·68 ±15%	2·11	
4545·38	(0)	$4s\ ^4P_{3/2}$	$5p\ ^4P_{5/2}^0$	0·51	0·94	K: n.o.
4526·20	(30)	$4s\ ^2P_{3/2}$	$5p\ ^2P_{3/2}^0$	40·7 ±2%	50·0	H
4491·05	(10)	$4s\ ^2P_{3/2}$	$4p'\ ^2D_{3/2}^0$	4·53	5·48	?Bl ?λ (6)
4475·31	(15)	$4s\ ^4P_{3/2}$	$5p\ ^4D_{5/2}^0$	4·70 ±5%	8·47	Bl (7)
4469·37	(18)	$4s\ ^2P_{3/2}$	$5p\ ^2P_{1/2}^0$	12·2 ±7%	7·32	P (8)
4446·11	(4)	$4s\ ^4P_{3/2}$	$5p\ ^4P_{1/2}^0$	4·40	2·61	K: 50% (9)
4445·83	(4)	$4s\ ^4P_{1/2}$	$5p\ ^4D_{3/2}^0$	2·30	2·73	K: 50% (9)
4438·48	(20)	$4s\ ^4P_{5/2}$	$5p\ ^4P_{5/2}^0$	11·2 ±4%	19·9	P (10)
4403·03	(15)	$4s\ ^4P_{5/2}$	$5p\ ^4P_{3/2}^0$	6·48	7·54	K: 74·6% (11)
4402·58	(4)	$4s\ ^4P_{1/2}$	$5p\ ^4D_{1/2}^0$	4·91	2·86	K: 25·4% (11)
4390·38	(7)	$4s\ ^4P_{1/2}$	$5p\ ^2S_{1/2}^0$	7·58	4·39	K: 10·5% (12)
4389·76	(25)	$4s\ ^4P_{5/2}$	$5p\ ^4D_{7/2}^0$	12·9	29·9	K: 80·0% (12)
4387·55	(6)	$4s\ ^4P_{1/2}$	$5p\ ^4S_{3/2}^0$	3·43	3·96	K: 9·5% (12)
4379·90	(20)	$4s\ ^4P_{3/2}$	$5p\ ^4D_{3/2}^0$	10·3 ±6%	11·9	
4371·55	(5)	$4s\ ^4P_{5/2}$	$5p\ ^4D_{5/2}^0$	1·44	2·48	K: 22·6% (13)
4369·52	(15)	$4s\ ^4P_{1/2}$	$5p\ ^2D_{3/2}^0$	6·39	7·33	K: 59·7% (13)
4363·30	(20)	$4s\ ^4P_{3/2}$	$5p\ ^2D_{5/2}^0$	6·49 ±8%	11·1	
4337·80	(1)	$4s\ ^4P_{3/2}$	$5p\ ^4D_{1/2}^0$	2·62	1·48	K: n.o.
4323·35	(20)	$4s\ ^4P_{3/2}$	$5p\ ^4S_{3/2}^0$	11·5 ±4%	12·9	
4305·55	(1)	$4s\ ^4P_{1/2}$	$5p\ ^2D_{3/2}^0$			E
4280·43	(2)	$4s\ ^4P_{5/2}$	$5p\ ^4D_{3/2}^0$	1·59	1·75	K: n.o.
4264·59	(5)	$4s\ ^4P_{5/2}$	$5p\ ^2D_{5/2}^0$	1·64 ±12%	2·68	
4226·44	(15)	$4s\ ^4P_{5/2}$	$5p\ ^4S_{3/2}^0$	6·06	6·50	K: (14)
4209·68	(12)	$4s\ ^4P_{5/2}$	$5p\ ^2D_{3/2}^0$	4·10 ±10%	4·35	
4147·20	(2)	$4s\ ^4P_{3/2}$	$5p\ ^2P_{1/2}^0$	3·83 ±14%	1·98	
4104·78	(3)	$4s\ ^4P_{5/2}$	$5p\ ^2P_{3/2}^0$	2·00	2·02	K: n.o.

(1) K, result depends on use of Kiess's data in some way; n, not measured; n.o., not observed here; B, broad; Bl, blend; %, line in question is about the stated % of the total measured strength of the blend, using K intensity and figure 2 (which was derived using *only* unblended Cl I lines); H, measured by Hey; E, error in classification; ?λ, anomalous behaviour, possibly λ-displacement; P, poor agreement between K and F intensities. (2) Cl II Bl 5099·30 (100 KB) probably negligible here. (3) Interference by H_β. (4) Bl Cl II 4819·46 (200 KB) and Cl I 4818·42 q.v. (5) Bl Cl II 4794·54 (250 KB). (6) ?Bl Cl II 4490·00 (50 KB) negligible here. (7) Bl Cl II 4475·28 (20 KB) negligible here. (8) $I_F = 0{\cdot}55\ I_{K-F}$. (9) Bl Cl I 4445·83 q.v. (10) $I_F = 1{\cdot}55\ I_{K-F}$. (11) Bl Cl I 4402·58 q.v. (12) Bl Cl I 4389·76 and 4387·55 q.v. (13) Bl Cl I 4369·52 and C I 4371·33 which has about 17·5% of the total intensity observed. The C II lines hereabouts are very weak in our source. (14) Weak Ca I 4226·728 bl. In the above notes, F refers to the present work, KB to Kiess and de Bruin (1939) and K–F to values given by Kiess corrected to absolute intensity by use of figure 2 of this work.

Table 3

Cl II Transition Probabilities, A_n^m and gf-values

λ (Å)	Intensity K and de B	Transition K and de B n	m	$10^{-8}\ A_n^m$ (A_n^m in sec^{-1})	$\lvert gf \rvert$	Notes
5423·25	(150)	3d $^5D_4{}^0$	4p $^5P_3$	0·38	1·19	(1)
4819·46	(200)	4s $^5S_2{}^0$	4p $^5P_1$	1·32	1·38	(2)
4810·06	(225)	4s $^5S_2{}^0$	4p $^5P_2$	1·39 ± 7%	2·41	
4794·54	(250)	4s $^5S_2{}^0$	4p $^5P_3$	1·47 ± 30%	3·55	(3)
5217	(75)	4s $^3S_1{}^0$	4p $^3P_{0,1,2}$	0·58 ± 20%	2·1	(4)

(1) What is actually observed includes λ 5423·52 and λ 5424·36 (for which allowance has been made using LS coupling intensities); (2) Bl Cl I 4818·64 (2K) = 29·4% and Cl I 4818·42 (3K) = 33·8% of total, whence 4819·46 has 36·7% of total; (3) log mean used to obtain A_n^m here, Bl Cl I 4796·76 (2K), which has 20·7% of total intensity; (4) components included here are 5217·93 (150) and 5221·34 (75). K and de B, Kiess and de Bruin (1939).

§ 5. DISCUSSION

5.1. *C I Transition Probabilities*

Excepting λ 5040 (see I), the new data in table 1 column (5) agree well with the previously recommended means in column (6); it is questionable whether these differ significantly from the new recommended means in column (7). This result is the best that could have been hoped for, but there is a disturbing scatter amongst the very careful measurements from different experiments.

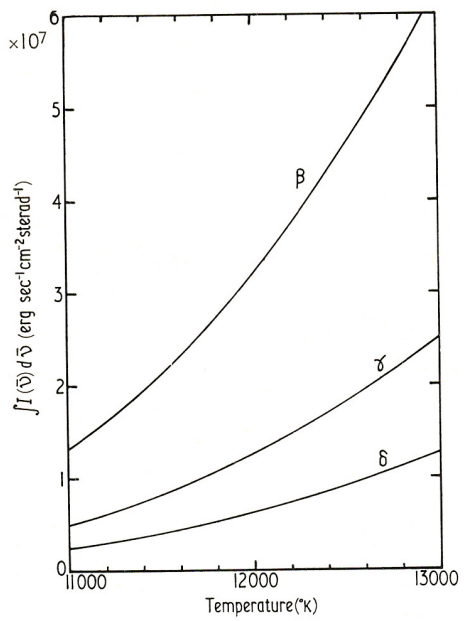

Figure 4. Absolute intensities of hydrogen lines as a function of temperature for an 18·5 mm long plasma column.

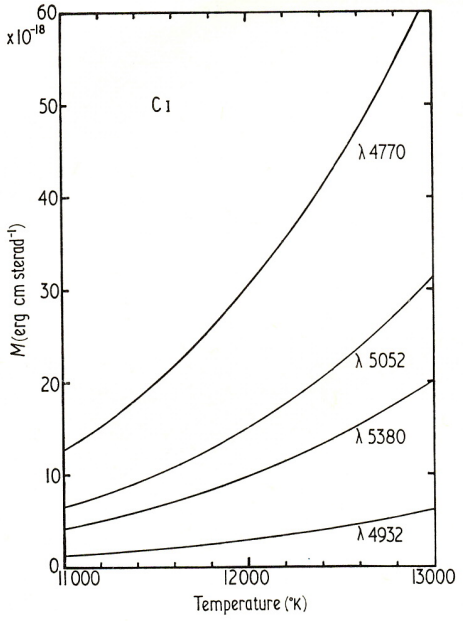

Figure 5

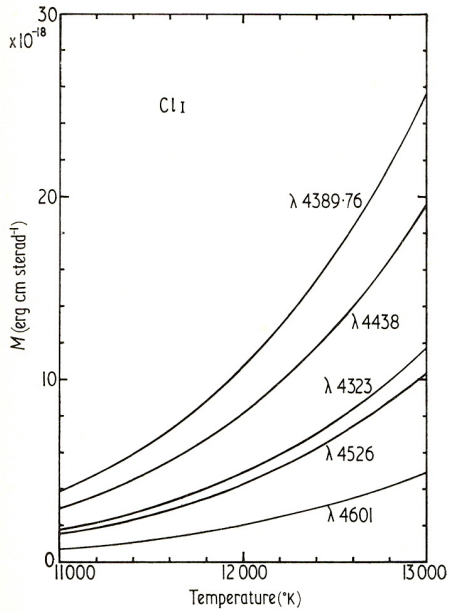

Figure 6

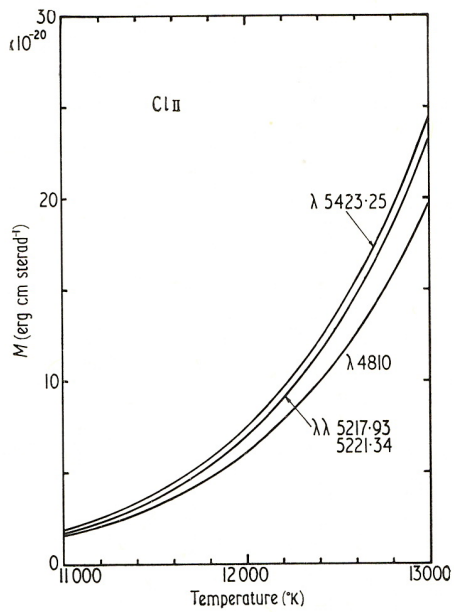

Figure 7

Figures 5, 6 and 7. The variation of computed M with temperature for C I, Cl I and Cl II lines respectively, where

$$M = \frac{\int I(\bar{\nu})d\bar{\nu}}{A_n{}^m n^P} = \frac{1}{4\pi}\frac{g_m}{Z}\exp\left(\frac{-E_m}{kT}\right)hc\bar{\nu}l$$

($n^P = n_N{}^C$, $n_N{}^{Cl}$ or $n_i{}^{Cl}$). These and similar curves together with a knowledge of the absolute intensities and gas temperature (hence the particle densities n^P from figure 3) made the transition probability determinations possible. Conversely, such (M, T) curves should become useful tools for chemical analysis of any uniform optically thin plasma column by absolute intensity measurements when the transition probabilities and the temperature are known. Transition probabilities are thought to be well measured for the selected lines. These figures refer to an l = 18·5 mm long plasma column (not necessarily from chloroform).

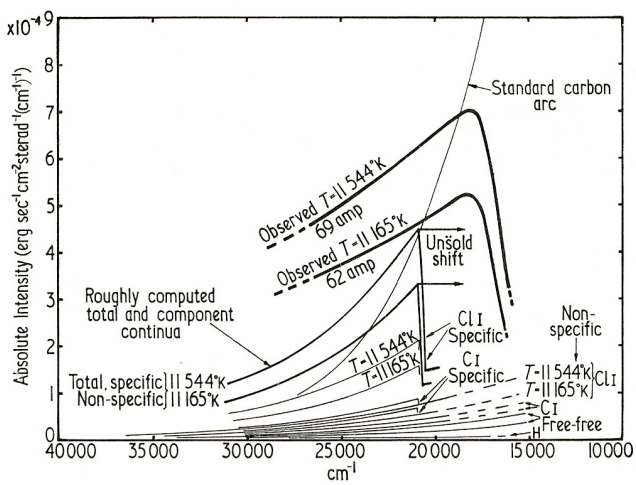

Figure 8. The chloroform continuum. Plasma column l = 18·5 mm.

5.2. *Cl I Transition Probabilities*

Hey's (1959) Cl I measurements are compared below with the new data which average systematically 23% greater.

λ (Å)	$10^{-6} A_n{}^m$ Hey†	$10^{-6} A_n{}^m$ Foster‡	$\frac{A_n{}^m \text{ (Foster)}}{A_n{}^m \text{ (Hey)}}$
4601	$3{\cdot}3_3 \pm 5\%$	$4{\cdot}21 \pm 3\%$	1·26
4326	$3{\cdot}2_3 \pm 5\%$	$4{\cdot}07 \pm 2\%$	1·26
4390	$1{\cdot}1_3 \pm 5\%$	1·29 Bl	1·14

† Tolerances are 'average errors'.
‡ Tolerances are probable errors from scatter.

Excluding the vacuum region the strongest Cl I multiplets lie in the infra-red as yet unmeasured.

5.3. *Cl II Transition Probabilities*

Observationally the Cl II lines were weak and sometimes blended with stronger Cl I lines. Nevertheless these few Cl II observations comprise the strongest Cl II multiplets, possibly excluding some in the vacuum region.

λ 4795, blended in our case, was previously measured by Hey. It is satisfactory that our value is again 23% above his.

Assuming Russell–Saunders coupling, absorption oscillator strengths of some *complete* multiplets can be derived:

Transition (Kiess and de Bruin 1939)	Absorption oscillator strength
$3s^2 3p^3 4s\ {}^3S^0 - 3s^2 3p^3 4p\ {}^3P$	0·70
$3s^2 3p^3 4s\ {}^5S^0 - 3s^2 3p^3 4p\ {}^5P$	1·47
$3s^2 3p^3 3d\ {}^5D^0 - 3s^2 3p^3 4p\ {}^5P$	0·66

The corresponding $^5S^0 - {}^5P$ transition in O I, namely $2s^2 2p^3 3s\ {}^5S^0 - 2s^2 2p^3 3p\ {}^5P$ was measured by Jurgens (1954) who also found a very large oscillator strength namely 1·7 against 0·919 calculated on the basis of *LS* coupling and the Bates and Damgaard (1949) tables.

5.4. *The Continuum*

To find the origin of the continuum the following have been estimated provisionally: (i) free–free continuum from all types of positive ion H^+, C^+ and Cl^+; (ii) continua from recombinations yielding high H, C I and Cl I states and contributing non-specifically to the obvious hump; (iii) continua from recombinations yielding lower C I and Cl I states and contributing specifically to the hump.

(i) the free–free absorption coefficient was computed from the Kramers–Gaunt–Cillié formula

$$K_{\bar{\nu}} = 1{\cdot}37 \times 10^{-23} \frac{g_u n_e n_i}{T^{1/2} \bar{\nu}^3} \tag{5}$$

(Allen 1955, p. 98) assuming only singly ionized hydrogen-like ions. If the total number of ions is n_i per cm^3

$$n_i = n_i{}^H + n_i{}^C + n_i{}^{Cl} \tag{6}$$

which is obtained from figure 3 for the two mean temperatures. The emission intensity

was then assumed to be given by Kirchhoff's Law

$$I_{\bar{\nu}} = B_{\bar{\nu}}(T)K_{\bar{\nu}}l \tag{7}$$

where $B_{\bar{\nu}}(T)$ is the Planck function and l is the length of plasma column.

(ii) The bound–free absorption coefficients for H were readily obtained from the Kramers–Gaunt formula (Allen 1955, p. 89) which can be put numerically

$$a_{\bar{\nu},n} = 1{\cdot}045 \times 10^{-2}\frac{g_{\mathrm{u}}}{n^5\bar{\nu}^3} \tag{8}$$

where $a_{\bar{\nu},n}$ is the photo-ionization cross section from the nth H level at wave number $\bar{\nu}$. We put the Gaunt factor $g_{\mathrm{u}} = 1$. This gives the absorption coefficient

$$K_{\bar{\nu},n} = \frac{g_n}{Z}n_{\mathrm{N}}{}^{\mathrm{H}}a_{\bar{\nu},n}\exp\left(\frac{-E_n}{kT}\right) \tag{9}$$

and again the intensity was obtained using Kirchhoff's Law, the $n = 3$, 4 and 5 levels contributing.

For the corresponding C I and Cl I components a gross approximation was made: the same formulae were used with E_n, n and g_n reinterpreted as the weighted mean energy E^*, the corresponding Rydberg denominator n^* and the statistical weight sums $g^* = \Sigma g_n$ for certain groups of states. The whole of the C I and Cl I energy level systems which could in any way contribute to 2 and 3 were divided up as follows (terms in the second and fourth sections contributing non-specifically):

Table 4

Spectrum	States (Moore 1949)	Statistical weight g_n	Energy E_n (cm^{-1})	Energy E^* (cm^{-1})	Term value (cm^{-1})	Rydberg denominator n^*†	Total weight g^*
C I	$3p\ ^1P$	3	68858				
	$3p\ ^3D$	15	69722				
	$3p\ ^3S$	3	70744				
	$3p\ ^3P$	9	71376	70234	20644	2·305	30
	$3p\ ^1D$	5	72611				
	$3p\ ^1S$	1	73976	72838	18040	2·466	6
	$2p^3\ ^3P$	9	75256				
	$3d\ ^1D$	5	77680	76122	14756	2·726	14
			78105–82252	79286	11592	3·076	103
			83500–88607	86297	4581	4·893	250
Cl I	$4p\ ^4P^0$	12	83060				
	$4p\ ^4D^0$	20	84159				
	$4s'\ ^2D$	10	84116				
	$4p\ ^2D^0$	10	84780				
	$4p\ ^2S^0$	2	85240				
	$4p\ ^2P^0$	6	85596				
	$4p\ ^4S^0$	4	85731	84310	20685	2·306	64
	$4p'\ ^2P^0$–$4d\ ^4D$	88	94310–95991	95199	19796	2·354	88
	$5p\ ^2P^0$–7	280	96309–101855	99024	5971	4·286	280

† From Fowler's (1922) table.

The non-specific contributions computed as indicated above are shown with thin lines on figure 8.

(iii) Specific contributions were sought as follows: with a knowledge of the electron density at a given temperature from figure 3, Unsöld's formula (4) gave an advance to the long wavelength of the series limit continua of 2698 cm^{-1} at $T = 11\,544$ °K and 2542 cm^{-1} at $T = 11\,165$ °K. This shift was added to the wave numbers of the observed humps at 18 200 and 18 250 cm^{-1} (respectively for $T = 11\,544$ and 11 165 °K) to give a mean $\bar{\nu}$, for an absorption edge undisturbed by microfields, at 20 845 cm^{-1}. The energy levels are thus obtained:

	H	C I	Cl I
Ionization potential (cm^{-1})	109 679	90 878	104 995
$\bar{\nu}$ edge (cm^{-1})	20 845	20 845	20 845
Energy level ± 1000 (cm^{-1})	88 834	70 033	84 150

For H, no levels contribute specifically but C I and Cl I levels tabulated in the first and third sections of table 4 will do so. This contribution was estimated roughly, as described under (ii).

The components and resultant emission are shown in figure 8. Under the action of the existing microfields, the hump will translate to the position indicated by the arrow. Owing to the allowed dispersion ($\pm 10^3$ cm^{-1}) of the levels contributing to the hump this will be broadened, but it is not profitable to investigate the shape in more detail in this crude approximation. Some of the difference between the observed and estimated continuum may be due to negative ions. The Cl^- spectrum, for example, should be very strong but it probably lies mainly to the short wavelength side of our region according to the electron affinity recommended by Massey (1950, pp. 19 and 21).

It thus appears that most of the continuum observed is the Cl I recombination spectrum with an appreciable contribution also from C I recombination. Some even more striking examples of similar application of Unsöld's formula have been demonstrated by Boldt (1961).

5.5. *Sources of Error*

The most unsatisfactory feature of this work is thought to be the absence of a direct measurement of axis wobble, which was impracticable at the time. It is reasonably certain from the type of noise observed in the time-resolved spectra and from the comparative sharpness of the plasma column, that the wobble was small. We have assumed that it was the same as that measured by Foster (1962) for arcs in steam. Whatever error this assumption causes (it could be 10%) it is unlikely that these Cl measurements suffer from systematic error more than the C I recommended means.

ACKNOWLEDGMENTS

The writer's thanks are due to Professor C. W. Allen for his continued support and to Professor P. M. S. Blackett and to Dr. R. W. B. Pearse and Dr. W. R. S. Garton for generous laboratory facilities at Imperial College. The Saha functions were computed by Mr. M. F. J. Britten.

REFERENCES

ALLEN, C. W., 1955, *Astrophysical Quantities* (London: Athlone Press).
BATES, D. R., and DAMGAARD, A., 1949, *Phil. Trans. Roy. Soc.* A, **242,** 101.
BOLDT, G., 1959, *Z. Phys.*, **154,** 319.
EULER, J., 1953a, *Ann. Phys., Lpz.*, **11,** 203.
—— 1953b, *Z. angew. Phys.*, **5,** 64.
FOSTER, E. W., 1958, *Proc. Inst. Electronics*, **3,** 2.
—— 1962, *Proc. Phys. Soc.*, **79,** 94.
FOWLER, A., 1922, *Report on Series in Line Spectra* (London: The Physical Society).
FRIE, W., and MAECKER, H., 1961, *Z. Phys.*, **162,** 69.
HEY, P., 1959, *Z. Phys.*, **157,** 79.
JURGENS, G., 1954, *Z. Phys.*, **138,** 613.
KIESS, C. C., 1933, *J. Res. Nat. Bur. Stand.*, **10,** 827.
KIESS, C. C., and DE BRUIN, T. L., 1939, *J. Res. Nat. Bur. Stand.*, **23,** 443.
MAECKER, H., 1951, *Z. Phys.*, **129,** 108.
—— 1953, *Z. Phys.*, **135,** 13.
—— 1956, *Z. Naturf.*, **11a,** 457.
MASSEY, H. S. W., 1950, *Negative Ions* (Cambridge: University Press).
MOORE, C. E., 1945, *A Multiplet Table of Astrophysical Interest* (Princeton: The Observatory).
—— 1949, *Atomic Energy Levels*, Vol. 1 (Washington: National Bureau of Standards).
RICHTER, J., 1958, *Z. Phys.*, **151,** 114.
—— 1961, *Z. Astrophys.*, **53,** 262.
UNSÖLD, A., 1948, *Z. Astrophys.*, **24,** 355.